SIN-CHN
SCIENTIFIC PRESS PTE.LTD.

Molecular & Cellular Biomechanics 2024, 21(4), 535.
https://doi.org/10.62617/mcb535

Article

Portable oxygen breathing apparatus integrated with biosensors: Enabling intelligent monitoring and optimal oxygen provision for biomechanical homeostasis

Honghao Zhang

Northwestern Polytechnical University, Xi'an 710072, Shanxi, China; leozhh@yeah.net

CITATION

Zhang H. Portable oxygen breathing apparatus integrated with biosensors: Enabling intelligent monitoring and optimal oxygen provision for biomechanical homeostasis. Molecular & Cellular Biomechanics. 2024; 21(4): 535. https://doi.org/10.62617/mcb535

ARTICLE INFO

Received: 14 October 2024
Accepted: 11 November 2024
Available online: 27 December 2024

Abstract: A lightweight, compact, inconspicuous gadget that provides extra oxygen when traveling is called a portable oxygen breathing apparatus. Cells rely on oxygen to drive the oxidative phosphorylation process within mitochondria, where adenosine triphosphate (ATP) is synthesized. Adequate ATP is essential for maintaining the muscle contraction and cell motility. With these portable devices, patients can maintain their oxygen therapy while going about their daily lives, enhancing their quality of life (QoL) and encouraging more mobility. An incorrect assessment could result in a low oxygen supply during exercise. Hypoxia-induced changes can also trigger intracellular signaling pathways that may lead to cell damage and, in the long term, contribute to the progression of various pathologies. Promising resolution to the difficulties can be discovered by incorporating machine learning (ML) algorithms and sophisticated monitoring systems into portable oxygen delivery devices. In this study, we propose a novel intelligent portable oxygen breathing apparatus integrated with biosensors (IPOBAB) that has revolutionized the treatment of long-term respiratory disorders, particularly severe hypoxemia and chronic obstructive pulmonary disease (COPD). IPOBAB system deployed with the Dynamic Gradient Boosting Machine (DGBM) classifier to classify the physical activities into low, moderate, and high exertion levels to ensure oxygen delivery is repeatedly adjusted based on the patient's current requirements. Inertial Measurement Unit (IMU) sensor data, blood oxygen saturation (SpO_2), and cardiovascular rate are just a few of the vital physiological features that biological sensors continuously monitor. This data lets doctors perform real-time assessments of a patient's health status. To eliminate noise, the information was processed using a median filter. The Fast Fourier Transform (FFT), which displays dominating frequency components, divides the electrical signal into individual frequencies to extract features. The results demonstrated that the IPOBAB model exhibits a high weighted accuracy of 98.4% in mechanically adjusting oxygen flow according to medical criteria compared to existing algorithms. This indicates that the system is effective in optimizing oxygen delivery, which is essential for maintaining the proper cell and molecular biomechanical functions in patients with long-term respiratory disorders. In conclusion, the IPOBAB represents a significant advancement in portable oxygen therapy as it combines adaptive oxygen delivery and comprehensive monitoring, thereby optimizing the care for patients with long-term respiratory conditions and safeguarding the integrity and functionality of cells and tissues at the molecular level.

Keywords: portable oxygen breathing apparatus; biosensors; inertial measurement unit (IMU); oxygen supply; dynamic gradient boosting machine (DGBM)

1. Introduction

Oxygen therapy has been shown to increase patients' survival rates in cases of severe hypoxemia and chronic obstructive pulmonary disease (COPD) since the

1980s. For COPD patients, long-term supplemental oxygen therapy (LTOT) is especially important because 47% of them have desaturation during exercise when their SpO_2 levels fall below 88%. By increasing O_2 saturation values above 90%, enhancing tissue oxygenation, postponing exacerbation and dyspnea, and boosting capacity for activity in COPD patients, LTOT seeks to prevent hypoxemia [1]. Children with pulmonary fibrosis also have a better quality of life (QoL) when exercise oxygen therapy is used. For doctors, caregivers, service providers, and individuals, however, the accompanying technology can be difficult, especially when it comes to prescription, titration, and equipment installation and administration. Closed-loop oxygen delivery methods haven't been adopted into normal scientific medical performance, despite worldwide recommendations demanding an effort and stress assessment for oxygen deprivation diagnosis at activity and calibration of blood oxygen levels needed for correction [2]. The Coronavirus Disease 2019 (COVID-19) pandemic has raised the need for medical oxygen supplies dramatically; yet, oxygen is lost greatly when oxygen cylinders and concentrating systems are used continuously for breathing. The four stages of the human breathing cycle are inhalation, breathing out, and exhalation pause [3]. About 25% of the breathing cycle is devoted to inhalation, with the rest 75% being made up of exhalation, inhalation pause, and exhale. Because humans only breathe in, there is a 75% loss of oxygen in the surrounding air. It is crucial to limit the oxygen delivery to subjects to inhalation exclusively to preserve medically necessary oxygen throughout the pandemic. One tactic to support the effective use of oxygen is the delivery of breathable air bolus via pulse mode [4]. The rise in healthcare demands for convenience and accessibility has led to funding initiatives for urban hospitals to address medical needs. The IoT has shown promise in the medical sector by enhancing technology and reducing costs. Biomedical IoT helps monitor, control, recognize, and act on systems, reducing medical costs. IoT-enabled wearables, embedded in the body, worn with additional devices, painted or affixed to the skin, or incorporated into clothes and accessories, have become essential components of IoT technology [5]. The use of technology in biomedical has grown essential due to the rise in demand for real-time monitoring of health, disease prediction, and fitness tracking. A market for wearable, adaptable sensors that can instantly identify and record physiological signs without the need for bulky, connected gear has resulted from this. By alerting users to aberrant health, these continual human information indicators enable preventive action. Nonetheless, there is little chance of qualitative gains in bio-functionality for many sensors intended for real-world use [6]. Signal processing is a field of the field of electrical engineering that deals with sound and pictures. Typical healthcare imaging methods that include processing signals are Magnetic Resonance Imaging (MRI), Computed Tomography (CT) scans, and X-rays. Speech noise is decreased by the use of digital signal processing. Bio-signals can be measured using numerous methods such as electrooculograms (EOG), electroencephalograms (EEG), electrocardiograms (ECG), and Electromyography (EMG). Sensors or biological markers, such as those based on sweat, tears, saliva, implants, arm adjustments, mouth cavity police officers, or foot mountings, are used in wearable biosensors to track health [7]. Although there have been considerable advancements in medical wearable devices, the range and caliber of vital signs they

offer are still limited. Respiration is a critical sign of a patient's decline, yet the miniaturization of respiration-sensing devices has been sluggish. In 2020, COVID-19 was the main cause of early mortality. Wearable technology in conjunction with a conducive setting for ongoing, remote monitoring of respiratory parameters can enable early symptom identification and prompt medical care, thereby lowering mortality. Ventilation and oxygenation are examples of respiratory functions, and assessing respiratory efficiency and oxygenation necessitates a thorough examination of numerous factors [8].

The objective of this research is to create an intelligent portable oxygen breathing apparatus that is integrated with biosensors (IPOBAB) to optimize the delivery of oxygen through adaptive monitoring. The device classifies degrees of physical activity and modifies oxygen flow based on the results using machine learning techniques, notably Dynamic Gradient Boosting Machine (DGBM). By guaranteeing a sufficient supply of oxygen at different levels of effort, this innovation improves the standard of care for individuals with chronic respiratory disorders.

Contributions of the study

- Innovative Device Design: Real-time monitoring and adaptive oxygen delivery systems are two features that the Intelligent Portable Oxygen Breathing Apparatus Integrated with Biosensors (IPOBAB) offers to recover portable oxygen therapy.
- Advanced Monitoring Capabilities: The incorporation of biological sensors provides the ongoing monitoring of vital physiological indicators, including heart rate and saturation of oxygen in the blood (SpO_2), enabling immediate evaluations of the patient's circumstance.
- ML Application: When influencing physical activity levels, the Dynamic Gradient Boosting Machine (DGBM) improves treatment outcomes for patients with chronic respiratory illnesses. This is so that oxygen administration can be adjusted automatically according to the patient's current level of effort.
- Enhanced Patient Safety and QoL: The IPOBAB greatly lowers the risk of hypoxemia and encourages greater independence among individuals by making sure they receive enough oxygen during various activities. This improves the overall QoL for people with persistent respiratory conditions.
- Data Processing Techniques: The use of advanced data preprocessing methods, such as median filtering and Fast Fourier Transform (FFT) for feature extraction, enhances the accuracy of physiological monitoring and supports the effectiveness of the device in clinical settings.

The next portions of this article are Portion 2: a literature review of this work, Portion 3: material and methodology, Portion 4: result with discussion, and Portion 5: conclusion.

2. Literature review

Concerning [9] suggested a system that will prevent hypoxia in patients by giving them extra oxygen during the COVID-19 pandemic. The patient's oxygen

consumption is monitored by the system through a cardiac sensor, which can result in hypoxia. The Arduino Uno uses a sensor that senses temperature to measure body temperature and a relay to control the necessary oxygen supply to operate a solenoid valve. Intranasal oxygen supply is accomplished via portable oxygen cylinders, and data is shown on a liquid crystal display. In addition, the system has a buzzer to notify the user in the event of a disaster and utilizes Global System for Mobile Communication (GSM) for non-emergency communication. This technology allows for flexible movement, is portable, and does not interfere with patients' lifestyles. Patients with less serious diseases can utilize the device at home or in hospitals. The work of [10] utilized machine learning (ML) and the Internet of Things (IoT) to monitor smart health to prevent these premature deaths. The suggested system has blood pressure sensing modules, temperature sensor sensors, pulse oxygen sensors, and a Thing Speak cloud for emergency communication with clinicians. Microcontrollers such as the Arduino Uno and Raspberry Pi are interfaced with these sensors. Using the IoT, the system continuously watches patients' data and updates it on Liquid Crystal Display (LCD) and doctor web pages. Both common and serious illnesses, such as lung disease and hypertension, can be predicted by a trained ML model. Patients with lung illness and heart attacks can't die suddenly from this method. In real-time circumstances, this method's accuracy is about 86%. Additionally, the work helps physicians follow patients remotely during pandemics like COVID-19. A noninvasive wearable gadget that leverages IoT to continuously monitor the health of a person was recommended by the research [11]. In addition to patient fall detection, the gadget measures arterial pressure, respiration rate, glucose levels, oxygen saturation, and temperature of the body, ECG, and location parameters. Moreover, it consumes a breath analyzer that measures the quantities of ammonia, dioxide of carbon, alcohol, sulfate of hydrogen, and transient organic compounds (TVOC) in breath. The system makes use of sensors and an 8-bit microcontroller that is connected through wifi to an internet-based information system. During surveillance from afar, the system also has a smartphone app called Role-based having access and an online dashboard. This innovative remote patient monitoring device is highly valuable for persistent illness patients in particular during the pandemic. A single system for controlling COVID-19 patients utilizing Long Range Wide Area Network (LoRaWAN) infrastructure for communication has been described in the publication [12]. For people who are confined or secluded, the technology enables remote surveillance of their health and symptoms without requiring external assistance. In addition to tracking the patient's present position, the IoT wearable measures vital signs like body temperature, the saturation level of oxygen, and pulse. After monitoring the two quarantined patients for 14 days, an actual Polymerase Chain Reaction (RT-PCR) test was achieved to confirm Severe Acute Respiratory Syndrome Coronavirus-2 (SARS-CoV2) contagion in cases where detected values were abnormal. Numerous patients can be monitored at once on the customizable nature of the suggested approach. Local authorities can successfully apply this system to improve monitoring capabilities and prevent fatalities. The IoT has changed the field of medicine by enabling remote monitoring of patients' health problems, as demonstrated by the article [13]. It allows sharing of information and storage by connecting built-in gadgets to the internet. Home automation systems,

automatic door locks, and thief detection are a few examples of applications. IoT facilitates the detection of life-threatening circumstances and the start of appropriate care. In this regard, ESP32 is creating a method for tracking complicated patients. After processing data, the IoT platform shows the data uptake from neighboring devices in real time. This analytics solution improves remote monitoring, lowers hospitalization rates, and allows for accurate and efficient treatment. Article [14] utilized cloud computing and the IoT to create a remote health surveillance system. Patients can check their illnesses from home because of this system's continuous health data collection through a variety of connected sensors and gadgets. By promoting real-time contact between patients and medical professionals, the system intends to improve the quality of care, minimize stays in hospitals, and avoid re-admissions. Incorporating IoT into electronic healthcare systems (EHS) not only enhances treatment results but also gives customers the ability to actively manage their health. In the end, this work advances innovations in digital health that lead to improved patient management and healthcare delivery. Study [15] investigated the application of the commercial optoelectronic biosensing module MAX30102 in the monitoring of peripheral oxygen saturation and heart rates in the medical field. Continuous monitoring can be performed because of the device's IoT capabilities and ESP32 system-on-a-chip. An intuitive user interface and 3D printable anatomic enclosure were also designed. The gadget is an attractive choice for creating biological sensing medical devices because of its dependability and accessibility. The author of [16] assessed the Wireless Body Area Network (WBAN) protocol-based VySys wireless vital sign monitoring system's accuracy, effectiveness, and clinical value. The device is small, light, and low-power. Two ubiquitous wireless biosensor sensors and a gateway are part of VySys, which transmits vital signs continuously to the cloud, whereupon apps for clients retrieve and display the information. The five vital signs of heart rate, respiration rate, body temperature, saturation of oxygen, and systolic blood pressure were examined in contradiction of a commercial medical-grade device in clinical trials involving fourteen participants. Findings confirmed that VySys is a credible option for ongoing health monitoring, with enhanced accuracy and limits of convergence over current systems, as well as significant statistical correlation. The developments in wearable and implantable technologies, such as wearable biosensing, biosensing, and Artificial Intelligence (AI)-biosensing, have been collected [17]. Material innovation, bio-recognition components, signal gathering and conveyance, data processing, and intelligent decision systems are the key areas of concentration. The report also covers the limitations and prospects of AI biosensors afterward medicinal devices. An IoT-based remote monitoring system for arterial pressure, respiration rate, and oxygen saturation in the blood was developed and put into use with the article [18]. The sensor gathers, assesses, forecasts, and interprets medical information that is kept on the "ThinkSpeak" IoT platform. The gadget derives and measures the photoplethysmography (PPG) signal using a physiological sensor with an incorporated signal conditioning unit and an identical PPG signal. The PPG signal's advantageous parameters are factored in using a computer-based algorithm. For remote health monitoring, the sensor can be connected to the Arduino 1010 WIFI MKR and worn as a ring sensor. The calculated SpO_2 readings are tracked remotely,

and a graphical depiction is created. The sensor's accuracy was assessed against two common commercially available measurement equipment. The application of wearable electromechanical displacement sensors based on laser-induced graphene (LIG) for the real-time monitoring of pulmonary signals in patients experiencing shock or respiratory distress was investigated in research [19]. A database of respiration signals, spanning from 86% to 100%, is created once the sensors are fastened to the subject's chest. An artificial neural network (ANN) framework is created for SpO_2 estimation using the database. In biosensing, incorporating mechanical respiration sensors and neural networks creates new opportunities for transparent SpO_2 surveillance. Surface electromyography (sEMG) data are used in the study [20] to automatically recognize instances of inhaling and exhalation, hence conserving medicinal oxygen. The device, called "RESPIPulse," is an intelligent pulse-based respiration device that does not require user intervention. By using ML techniques, the device seeks to reduce oxygen waste during the process of the exhalation phase and increase oxygen supply efficiency. It has been established that k-nearest neighbor (kNN) is the most accurate method for identifying respiratory occurrences. Extensive oxygen savings over current pulse-operated devices have been demonstrated in trials including both healthy volunteers as well as patients with dyspnea.

3. Methodology

In this research, we proposed a novel Intelligent Portable Oxygen Breathing Apparatus Integrated with Biosensors (IPOBAB) revolutionary system that integrates biosensors to provide oxygen therapy with optimized efficiency based on the user's oxygen needs in real-time, as depicted in **Figure 1**.

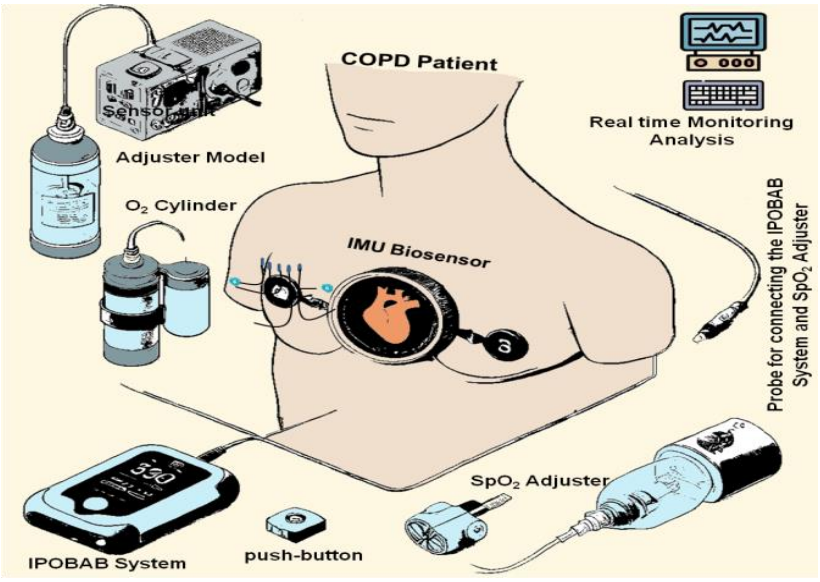

Figure 1. IPOBAB revolutionary system.

Initialization involves the system performing self-checks, utilizing Serial Peripheral Interface (SPI) pins to connect the Microprocessor Unit (MPU) 9250 Inertial Measurement Unit (IMU), pressure sensor, pulse oximeter sensor, and flow

sensor to the Microcontroller Unit (MCU) for measuring blood oxygen saturation (SpO_2) and pulse rate, which are key indicators for controlling the oxygen flow. A push-button pin connected to the General-Purpose Input / Output (GPIO) pins ensures accurate oxygen delivery based on the patient's activity level and health conditions. The IPOBAB hardware components include the oxygen concentrator unit, which filters and provides medical-grade oxygen from ambient air; a compressor that compresses and delivers air into the system; limestone filters that absorb nitrogen; and an oxygen tank that stores the separated oxygen for the user to inhale. The IPOBAB device features a 6-pin connector for personalized oxygen flow levels, with pins P1–P6 assigned for patient requirements, and a manageable O_2 concentrator interface for controlling oxygen flow and powering the control unit. The MCU, based on the ARM Cortex-M0 architecture, processes sensor input signals via a Tensor Processor Unit (TPU) to detect the patient's physical activity and movement patterns, using a Dynamic Gradient Boosting Machine (DGBM) to adjust the flow rate based on the user's SpO_2 levels and physical exertion. Initially, a median filter is utilized to remove noise from the input signals, and features extracted from the denoised signals are accomplished using Digital Signal Processing (DSP) techniques such as Fast Fourier Transform (FFT) to control oxygen delivery. It also includes built-in memory and supports an external µSD card for data storage; the overall functionality of this study is illustrated in **Figure 2**.

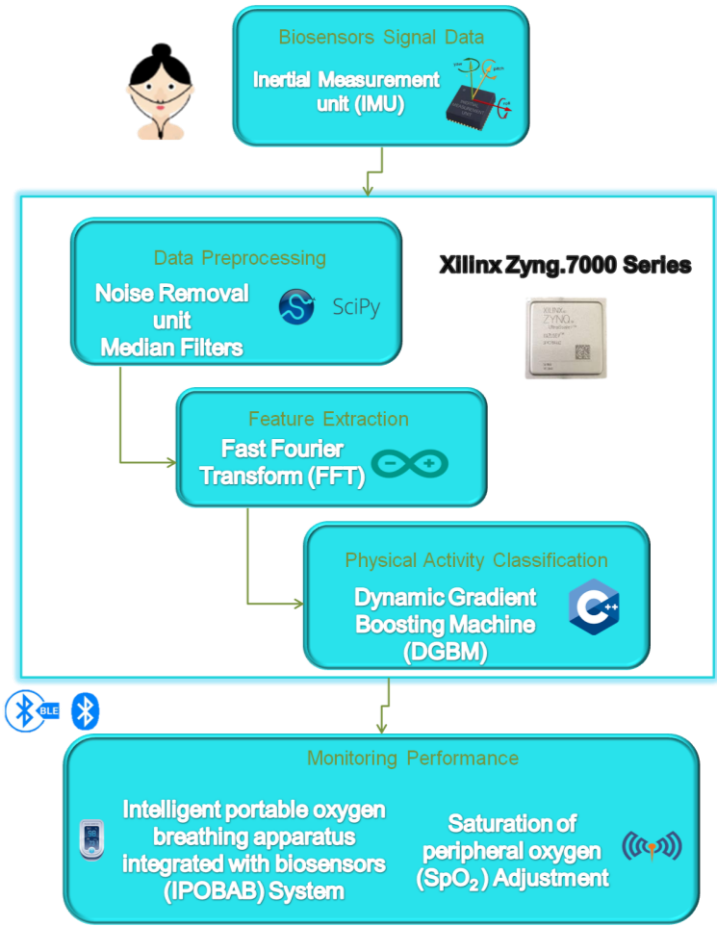

Figure 2. An overview of processes for methodology.

The IPOBAB is powered by a rechargeable 700 mAh lithium-ion battery, designed for several hours of continuous use, or can be powered through an external AC supply for long-term use at home. The IPOBAB runs using a Real-Time Operating System (RTOS) such as Linux Embedded C++, with an oxygen flow control algorithm implemented on the tensor processor model operating the overall IPOBAB system. A Bluetooth Low Energy (BLE) module connected to the Universal Asynchronous Receiver-Transmitter (UART) provides wireless connectivity for data transmission and allows remote monitoring through mobile applications, employing the Message Queuing Telemetry Transport (MQTT) protocol for oxygen flow control feed messaging in the User Interface (UI) port. If the user is exercising or if SpO_2 levels drop below a predefined threshold, the system boosts oxygen delivery, conversely, if the user's SpO_2 is within the normal range and they are resting, it reduces the flow rate to conserve battery power and oxygen. User feedback is provided through the mobile app, displaying current oxygen delivery, pulse rate, battery status, and system health. Alerts and notifications are issued via MQTT if SpO_2 levels fall below safe limits or if there is a malfunction with the concentrator. The IPOBAB system configuration modes are illustrated in **Figure 3**.

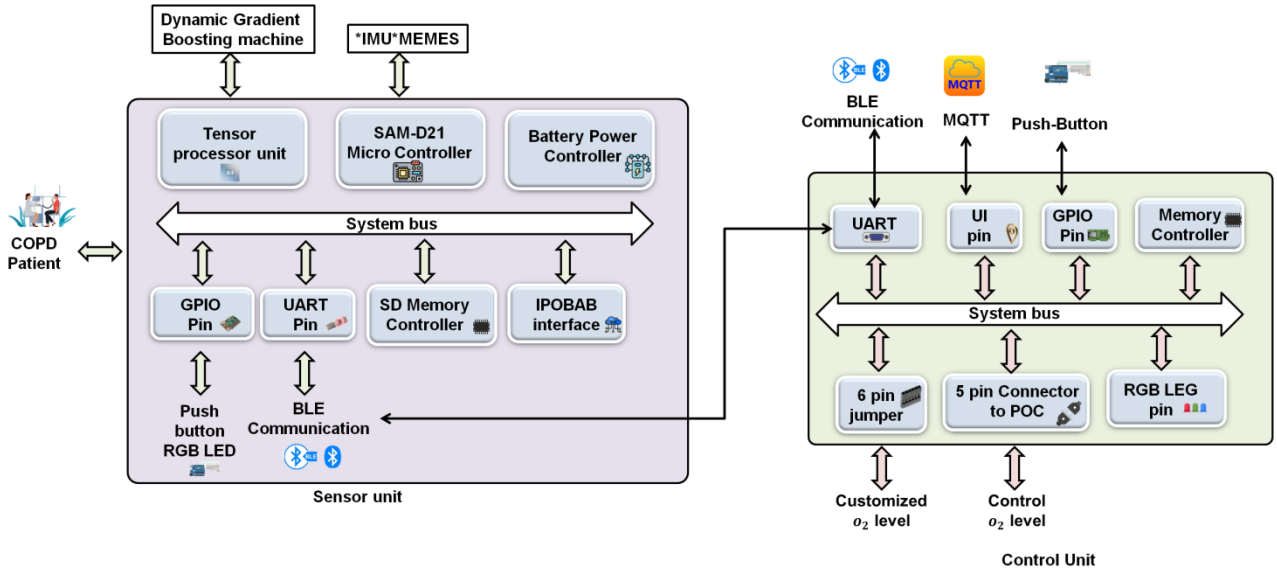

Figure 3. The configuration of the IPOBAB system.

3.1. Study design and participants

An outline of 25 research participants, including their demographics and other pertinent health-related data. It shows that 24% of the population is female and 76% of the population is male. Additionally, the age range of the group is 50–89 years old. The severity of dyspnea was indicated by the mean BMI of 26.8 ± 4.0 and the baseline degree of dyspnea as determined by the Modified Medical Research Council, which was 2.4 ± 0.6. Lower lung function is indicated by a FEV1/FVC ratio in the range of 0.52 ± 0.18.

In **Table 1**, activity level: 32% are low, 56% are medium, and 12% are high. SpO_2 level: 28% fall into the 85%–70% range, 24% fall below 70%, and 48% fall into the 86%–90% range. It varied between 81–90 bpm (8%), and less than 50 bpm

(32%). Three-quarters of patients are lowly active, fifty-six percent are medium active, and twelve percent are highly active. 48% of patients had SpO_2 values between 86 and 90%, 28% have levels between 85%–70%, and 24% have levels below 70%. The heart rate reflects the variety in cardiovascular response, ranging from less than 50 bpm (32%) to 81 bpm–90 bpm (8%). 52% of patients need 3 L/min–6 L/min of oxygen, whereas 48% of patients need 1 L/min–3 L/min. Furthermore, the LTOT history is 24.3 ± 15.8 months, and the average daily POC usage duration is 2.5 h ± 1.2 h.

Table 1. Demographic characteristics of the COPD patients.

Characteristics data		**Value**
Number of Patients		*N* = 25
Gender	Male	19 (76.0%)
	Female	6 (24.0%)
Age	50–59	3 (12%)
	60–69	8 (32%)
	70–79	5 (20%)
	80–89	9 (36%)
Body Mass Index (Kg/m^2)		26.8 ± 4.0
Modified Medical Research Council dyspnoea baseline level		2.4 ± 0.6
Forced Expiratory Volume in 1 second to Forced Vital Capacity ratio		0.52 ± 0.18
Daily hours using the POC		2.5 ± 1.2
LTOT history (months)		24.3 ± 15.8
Activity Level	Low	8 (32%)
	Medium	14 (56%)
	High	3 (12%)
SpO_2 Level	86–90	12 (48%)
	85–70	7 (28%)
	Below 70	6 (24%)
Heart Rate (bpm)	81–90	2 (8%)
	80–71	4 (16%)
	70–61	7 (28%)
	60–51	4 (16%)
	Below 50	8 (32%)
Oxygen Flow Rate (L/min)	1–3	12 (48%)
	3–6	13 (52%)

Then to gather data from actual activities, participants were asked to walk and climb stairs. The length of the exercise, the use of POC, oxygen flow levels, the saturation of oxygen, heart rate, and distance taken to walk were among the variables that the researchers noted. The energy cost of physical activity was measured using the metabolic intensity of operations (MIO). Because COPD patients rarely engage in high-intensity exercise, the study concentrated on low- to moderate-intensity activities are illustrated in **Table 2**. It represents the various activities that COPD

patients are engaged in, categorized by intensity. The intensity is sedentary, light, moderate, and vigorous. MIO values and the corresponding number of cases are also given. The table is used to estimate energy expenditure in different physical tasks and helps guide oxygen adjustments based on activity levels. To make sure patients received the appropriate amount of oxygen, medical professionals modified the amount of oxygen required from the POC according to each patient's activity intensity.

Table 2. Presents the classification of activity intensity.

Performance	Activities	MIO	Quantity of cases
Sedentary	Sitting	1.3	2160
	Standing	1.5	1389
	Lying	1.0	1592
Light	Walking	2.1	3115
	Light housework	2.5	1505
Moderate	Walking upstairs	3.5	809
	Walking downstairs	3.9	763
	Gardening	4.1	502
Vigorous	Running	7.0	382
	Cycling (fast pace)	8.0	201
	Aerobic exercises	6.5	490
Total			12,908

IMU sensor captures data about analyzing COPD patients' SpO_2 levels, heart rate, and oxygen flow rates during daily activities. This study includes activities like eating that require moving your hands or walking. Mobile devices such as wrist straps and elastic waistbands can be paired with smartphones. The three directions of the accelerometer, magnetometers, and gyroscope data from the device that is worn are used to calculate *x*, *y*, and *z* (see **Figure 4**).

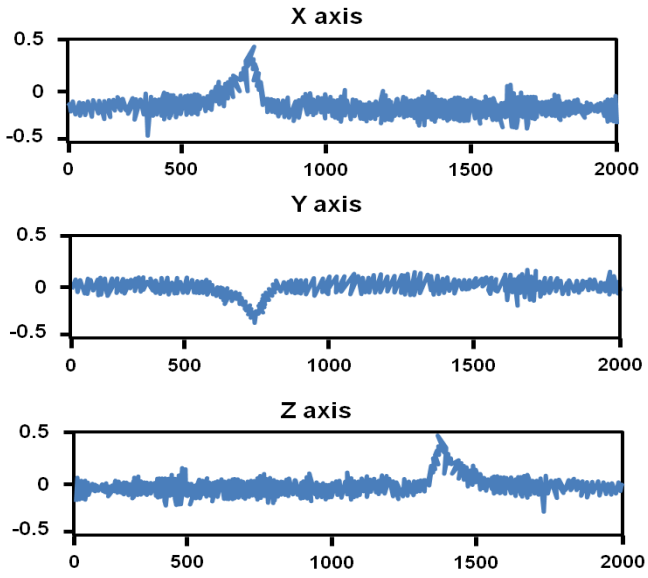

Figure 4. Displays raw IMU signal data before processing.

3.2. Data preprocessing using median filter

The median filter is applied to remove unwanted noise from the IMU sensor data collected from the patient's activity, specifically in the *x*, *y*, and *z*-axis signals. The IMU captures accelerometer, magnetometer, and gyroscope data, which could include signal distortions due to the patient's movements or environmental factors. By using the median filter, each data point in the sliding window is replaced with the average value of the bordering points, successfully pressing the signal though retaining essential details, such as rapid changes in motion that indicate activity transitions are illustrated in **Figure 5**.

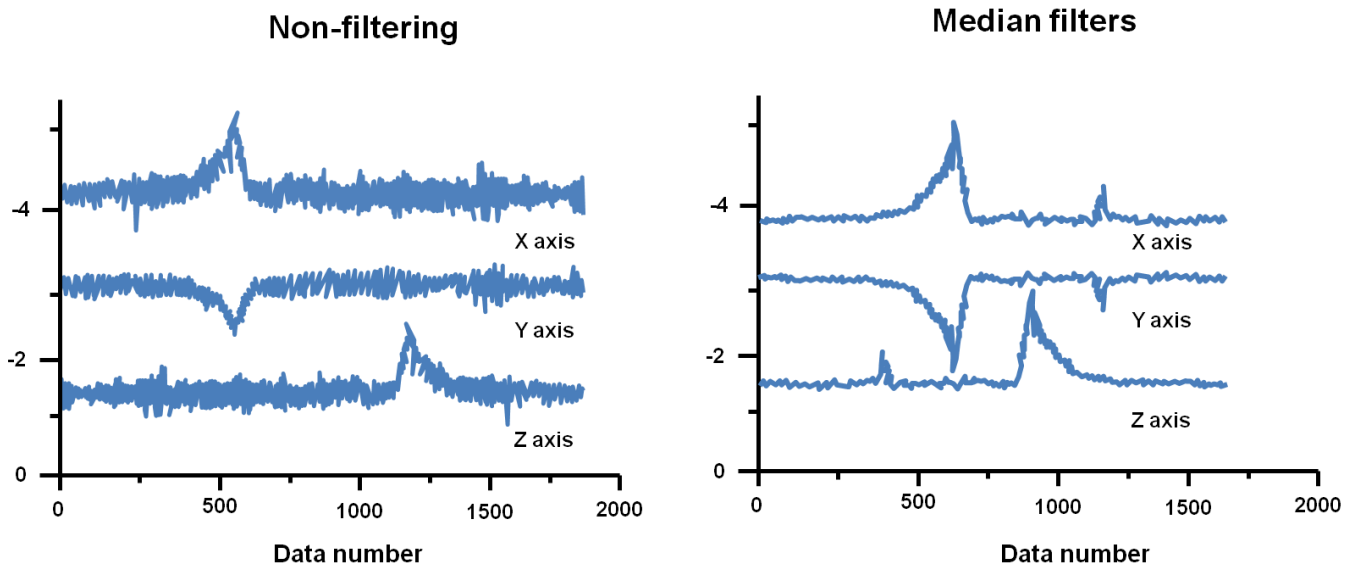

Figure 5. Demonstrates the noise removal mechanism applied to IMU data.

This method helps preserve critical features of the patient's movements and ensures more accurate detection of activity patterns without losing important signal details during noise suppression.

We refine the transmittance optimization process for improved patient activity recognition by integrating median filtering into the IMU data analysis. Let the window size $\Omega(w,z)$ *be* $M \times M$, where $X(w,z)$ is calculated using the minimum and maximum values of J_{min}, as shown in Equation (1):

$$X_{(w,z)} = \begin{bmatrix} \min\limits_{(w,z)\,\in\Omega(w,z)} J_{min}(w,z) \\ \max\limits_{(w,z)\,\in\Omega(w,z)} J_{min}(w,z) \end{bmatrix} \quad (1)$$

here, (w,z) denotes the pixel coordinates, and J_{min} represents the minimum frequency value. The minimum and maximum values within the window are denoted as $X_{(w,z)}(M^2-1)$ respectively. The dark channel prior (DCP) value $I_{dark}(w,z)$, for noise reduction in signal processing, is expressed in Equation (2):

$$I_{peak}(w,z) = X_{(w,z)}(0) \quad (2)$$

The DCP calculation can be modified by applying a median filter, as described in Equation (3):

$$I_{peak}(w,z) = \underset{(w,z)\in\Omega(w,z)}{\text{med}}\left(\min_{d\in(q,h,a)} I^d(w,z)\right) \tag{3}$$

Given that the vector $X_{(w,z)}$ is ordered from smallest to largest, the refined peak values of the signal are computed by Equation (4):

$$I_{peak}(w,z) = X_{(w,z)}\left(\frac{M^2-1}{2}\right) \tag{4}$$

Replacing the original minimum filter with the median filter transforms the transmittance calculation into Equation (5):

$$s'(w) = 1 - \omega \underset{(w,z)\in\Omega(w,z)}{\text{med}}\left(\min_{d}\frac{J^d(w,z}{B^d}\right) \tag{5}$$

Finally, the denoised IMU signal for accurate patient activity recognition is derived through Equation (6):

$$I(w) = \frac{J(w)-B}{\max(s'(w),s_0)+B} \tag{6}$$

By integrating median filtering into the signal processing workflow, we enhance noise removal in the IMU data, yielding clearer and more accurate activity recognition for optimal oxygen flow control. At an average sampling rate of 25 Hz, both the accelerometer and gyroscope's (*X*, *Y*, and *Z*) data were gathered. It was thought that this division of the acceleration signals into periods of 3 s with no overlap would prove enough for recording the important aspects of the signal. Annotated labels allowed for the identification of processes at varying intensities.

3.3. Fast fourier transform (FFT) employed to feature extracting the IMU signal

The Fourier Transform is used to extract features after the median filter has been applied to eliminate noise in the IMU signal data (*x*, *y*, and *z* axes) and enable activity in patients' identification are depicted in **Figure 6**. Researchers can examine the recurrent frequency pattern that corresponds to the patient's activities by breaking down the filtered IMU signal into each of its frequency elements using the Fast Fourier Transform (FFT).

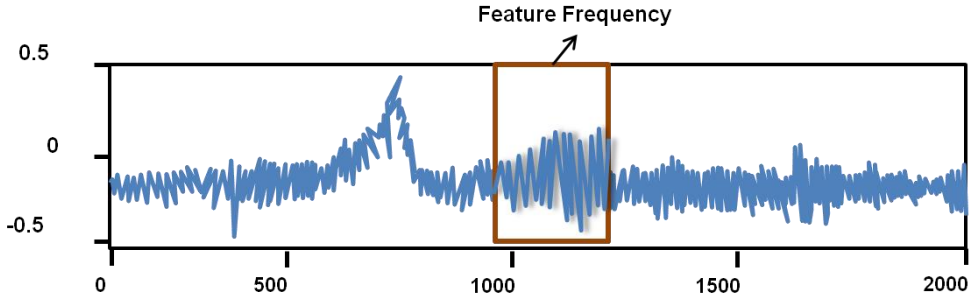

Figure 6. The refinement of activity patterns for feature extraction.

Consider that y_j represents a discrete signal that is output with a magnitude n and$m = 0, 1, 2, 3, .., M-1$. Following the FFT alteration, the result will be $y_{j,l}$ for

$j = 1, 2, 3, \ldots\ldots\ldots\ldots, n$ and $l = 0, 1, 2, 3, \ldots\ldots\ldots, a-1,$ where n the size of the samples is used for training and a is the unchanged harmonic size. The FFT can be obtained by:

$$W(l) = \sum_{m=0}^{M-1} w(m)\, X_M^{lm}, \tag{7}$$

$$l = 0,1, \ldots., M-1$$

$$X_M = f^{\frac{-i2\pi}{M}} \tag{8}$$

$$W(l) = \sum_{m\ even} w(m)\, X_M^{lm} + \sum_{m\ odd} w(m)\, X_M^{lm} \tag{9}$$

$$W(l) = \sum_{n=0}^{\frac{M}{2}-1} w(2N)\, X_M^{2lm} + \sum_{n=0}^{\frac{M}{2}-1} w(2N)\, X_M^{2lm} \tag{10}$$

With $X_M^2 = X_{M/2}$ substitution, the Equations (11) and (12) can be expressed as

$$W(l) = \sum_{n=0}^{\frac{M}{2}-1} g_1(n)\, X_M^2 + \sum_{n=0}^{\frac{M}{2}-1} g_1(n)\, X_{M/2}^2 \tag{11}$$

$$X(l) = G_1(l) + X_{M/2}^l G_2(l)\ l = 0,1, \ldots., M-1 \tag{12}$$

The $\frac{M}{2}$ position DFTs of the patterns $g_1(n)$ and $g_2(n)$, accordingly, are represented by the values $G_1(l)$ and $G_2(l)$ Period $\frac{M}{2}$ characterizes $G_1(l)$ and $G_2(l)$ consequently $G_1\left(l+\frac{M}{2}\right) = G_1(l)$ and $G_2\left(l+\frac{M}{2}\right) = G_2(l)$. In addition, the formula $X_M^{l+M/2}$, the equation can therefore be expressed as Equations (13) and (14).

$$W(l) = G_1(l) + X_M^l G_2(l), l = 0,1, \ldots, \frac{M}{2} \tag{13}$$

$$W\left(l+\frac{M}{2}\right) = G_1(l) - X_M^l G_2(l)\,, l = 0,1, \ldots\ldots, \frac{M}{2} \tag{14}$$

where N is the output discontinuous signal total number of points for sampling, these equations will be used to compute the input signal's FFT transform, which will demonstrate the activity signature in the domain of frequency.

3.4. Physical activity classification model using dynamic gradient boosting machine (DGBM)

Gradient Boosting Machine (GBM) is a form of assembly learning that builds uninterrupted decision trees to exploit prediction accuracy. It combines the consequences of weak learners to optimize. An improved form of GBM called Dynamic Gradient Boosting Machine (DGBM) animatedly modifies its learning in

reaction to broken-up patterns in the input data, mounting its receptiveness to time-dependent fluctuations such as physical activity. Its most important benefit is its capability to adapt the model in real-time situations, guaranteeing precise and appointed time forecasts under changing conditions such as enduring health monitoring. To successfully deal with the difficulties of disturbed signal data in patient activity level classification, we developing the DGBM method in this study. The approach uses a Bayesian model for hyperparameter optimization and the Fuzzy C-Means (FCM) method for sampling data sets with imbalances. We improve the signal data collection's quality and enable more accurate activity classification by adding a clustering algorithm. Moreover, feature selection aids in removing redundant attributes, which lowers the process of learning the algorithm's sophistication. The following are the DGBM approach's facilitates accurate classification of patient activity levels, ensuring that the model effectively distinguishes between various exertion levels for optimal oxygen delivery, the DGBM method's primary stages are depicted in Algorithm 1.

Algorithm 1 DGBM

Input: IMU Signal
Output: Classification results for patient activity levels (low ($f < 1$), moderate ($2 < f < 5$) and high ($F > 5$))
Step 1: Read original IMU signal data, frequency node, and standardize data features;
Step 2: Partition pre-processed signal data into Maximum frequency node B and Minimum frequency node A;
Step 3: Execute fuzzy C-mean for Maximum frequency node B, return the sampling signal data node D;
Step 4: Merge frequency mode C and Minimum frequency mode B into IMU signal data balance;
Step 5: Use gradient boosting algorithm for feature frequencies of IMU signal data balancing;
Step 6: Use GBM algorithm for construction tree based-classifier;
Step 7: Bayesian hyperparameter optimization;
Step 8: Operate optimal hyperparameter model to obtain classification results;
Return Classification patient activity levels (low ($f < 1$), moderate ($2 < f < 5$), and high ($F > 5$)).

Figure 7 depicts the iterative process of a DGBM in classifying physical activities based on feature frequencies into different levels of exertion. This process is crucial for regulating oxygen delivery in response to a patient's current exertion level. In each iteration, the trees progressively adjust the boundaries, improving the classification of activities into low ($f < 1$), moderate ($2 < f < 5$), and high ($F > 5$). As more trees are added, the DGBM refines the output, providing more accurate predictions of exertion levels, and ensuring oxygen delivery is more precisely adjusted to meet a patient's needs. In algorithm 2 C denotes the values of the signal frame, and B and D are the activity status of the patients. In **Figure 7** the circle share represents the activity state and the square shape illustrates the inactivity status of the patient.

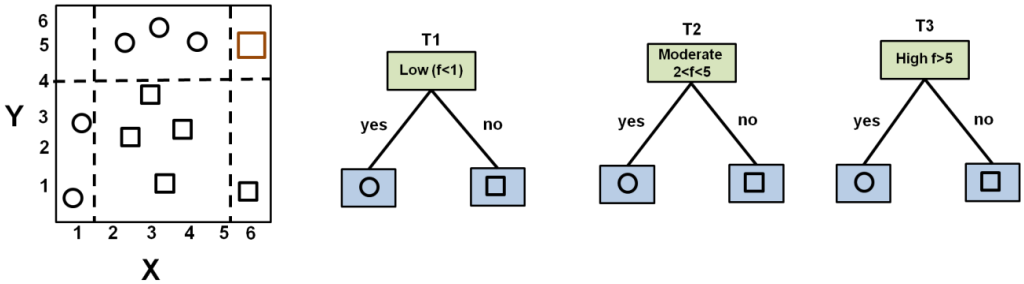

Figure 7. Introduces the DGBM activity identification model for accurate activity classification.

4. Result and discussion

Python 3.11 platform was used for the outcome research. A laptop running Windows 10 with an Intel i7 CPU and 32 GB of RAM is used to analyze the physical activity status of 25 COPD patients using DGBM. with three separate trees through 3276 nodes of low exertion, 3413 nodes of moderate exertion, and 550 nodes of high exertion made up the data set used in this study phase. **Figure 8** illustrates a test and the signals obtained over sometime during various activities. The experiment involved collecting signals from a patient while walking through a hospital test circuit. The IMU measured three types of signals; they are 3-axis accelerometer signals in **Figure 8a**, gyroscope signals in **Figure 8b**, and barometer signals in **Figure 8c**. The accelerometer signals measured the patient's movement in three directions, the gyroscope signals detected their body rotation, and the barometer signals measured air pressure changes. The red vertical lines in the signal plots indicated changes in activity, such as transitioning from level ground to stairs.

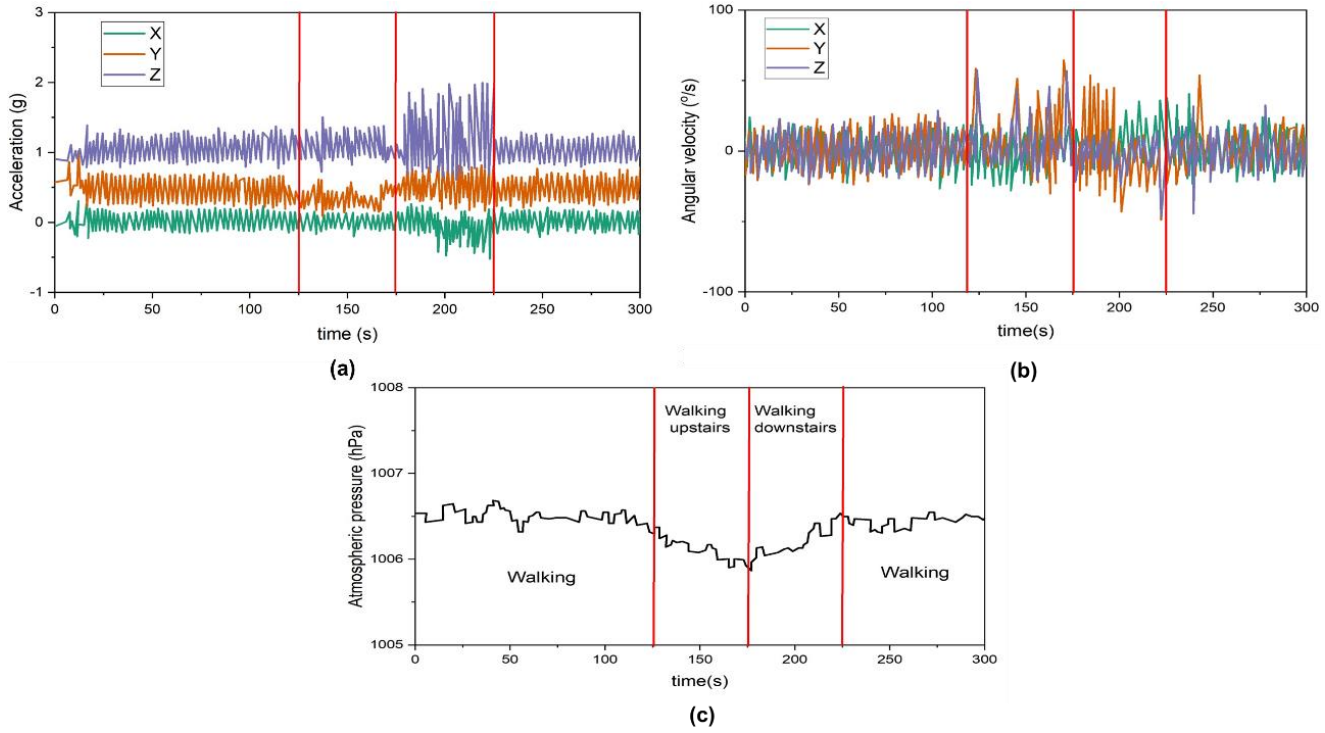

Figure 8. IMU Signal data includes three key components for activity tracking **(a)** accelerometer signals; **(b)** gyroscope signals for rotational motion; **(c)** barometer signals.

The IPOBAB integrated with a DGBM has demonstrated high performance and efficiency in managing oxygen delivery. The system's Weighted Accuracy was 98.4%, indicating its reliability in identifying patient activities and adjusting oxygen flow accordingly. SpO_2 levels averaged 94.5%, indicating healthy oxygen levels and preventing hypoxemia during physical activity. Heart rate was stable, with 78.3 beats per minute, ensuring patient safety. The Oxygen Flow Rate Adjustment ranged from 0.5 L/min to 6.0 L/min, dynamically adjusted based on real-time physiological data. Activity levels were divided into low, moderate, and high-intensity categories, allowing the DGBM to fine-tune oxygen delivery according to the patient's specific

needs; **Figure 9** depicts the DGBM classifier predicting the activity level of the COPD patients.

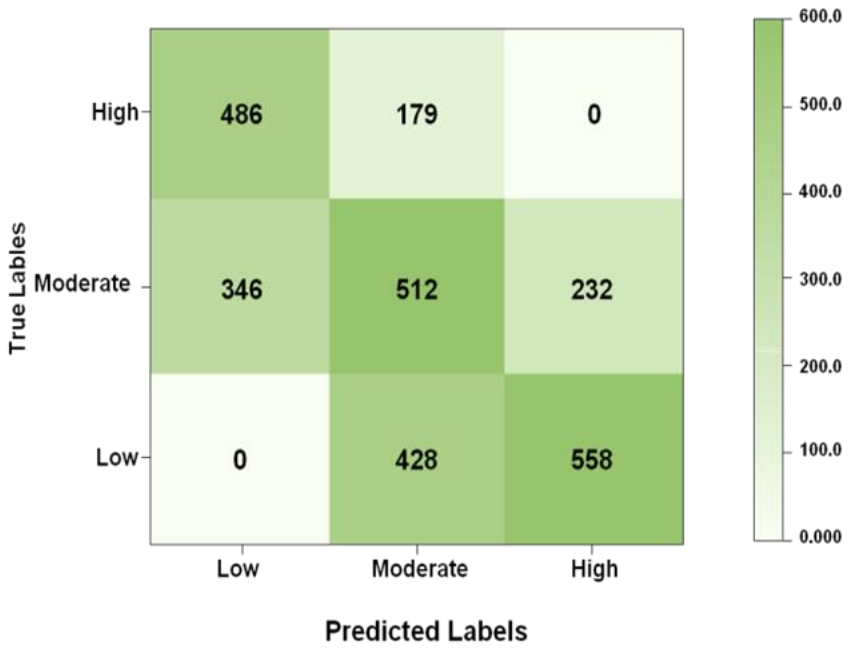

Figure 9. Visualizes the predicted outcomes from the classifier mode.

Patient satisfaction was high, with an average of 4.7, indicating comfort and effectiveness. The system led to a 40% Mobility Improvement, enhancing patients' ability to perform daily tasks compared to their baseline mobility before using the apparatus. Overall, the IPOBAB system effectively manages oxygen delivery, improves patient mobility, and maintains health standards during its use. The device attended a high accuracy performance level is influenced by inaccuracies in categorizing activities upstairs and downstairs, due to inherent difficulties and variations in patient walking patterns. Long flights of stairs are typically avoided by COPD and respiratory failure patients receiving LTOT, making these mistakes less critical in real-world situations. **Table 3** compares blood oxygen saturation variations for 7 COPD patients in traditional portable oxygen breathing apparatus integrated with biosensors (POBAB) and automatic IPOBAB tests. When comparing average oxygen saturation in the blood readings to standard testing, four out of seven COPD patients exhibited a decrease in desaturation occurrences and an improvement. When POBAB was utilized, the total amount of time spent without SpO_2 between 90% and 85% demonstrated improved responsiveness. Because of backache worsening, seven people with COPD reported decreased mobility, which could have an impact on the test outcomes. Reduced saturation in the time leading up to intensification has been seen by certain writers, which can indicate distortion in the examination's findings.

Table 3. Presents the response data of seven COPD patients.

Modes	**Traditional method**							**IPOBAB**						
Patients	P_1	P_2	P_3	P_4	P_5	P_6	P_7	P_1	P_2	P_3	P_4	P_5	P_6	P_7
SpO_2 events	2	4	3	6	4	2	4	2	1	1	3	2	1	1
Mean SpO_2 (%)	92.4	89.7	93.1	89.9	90.5	91.6	87.9	89.5	91.5	86.1	90.4	88.6	87.1	94.2
CT90 (%)	73.8	68.3	17.9	7.4	9.3	67	50.4	91.7	49.3	97.5	29.5	31.4	64.6	23.6
Max SpO_2 (%)	93	91	85	90	78	92	86	95	98	92	94	96	92	90
Oxygen Flow Rate (L/min)	2.0	2.4	2.1	2.7	2.3	2.2	2.5	3.7	3.2	2.9	3.8	3.0	3.5	3.9
CT85 (%)	32.6	12.6	0.00	0.00	0.00	29.4	0.00	9.6	0.00	7.2	12.8	0.00	32.6	14.6
Min SpO_2 (%)	77.9	76.9	73.9	89.4	85.7	88.7	84.6	80.9	69.7	79.6	81.0	95.9	97.4	89.7

One participant's change in their saturation of blood oxygen pattern throughout exertion is shown in **Figure 10**. It is evident that using the suggested method increased the mean value, stabilized SpO_2 levels, and decreased the amount of desaturation occurrences. A participant's SpO_2 patterns throughout the scientific experiment are shown in **Figure 10**. When utilizing a handheld oxygen concentrator in the suggested automated mode, the SpO_2 values are indicated by the yellow line. The SpO_2 readings measured with the IPOBAB in traditional mode are indicated by the green line.

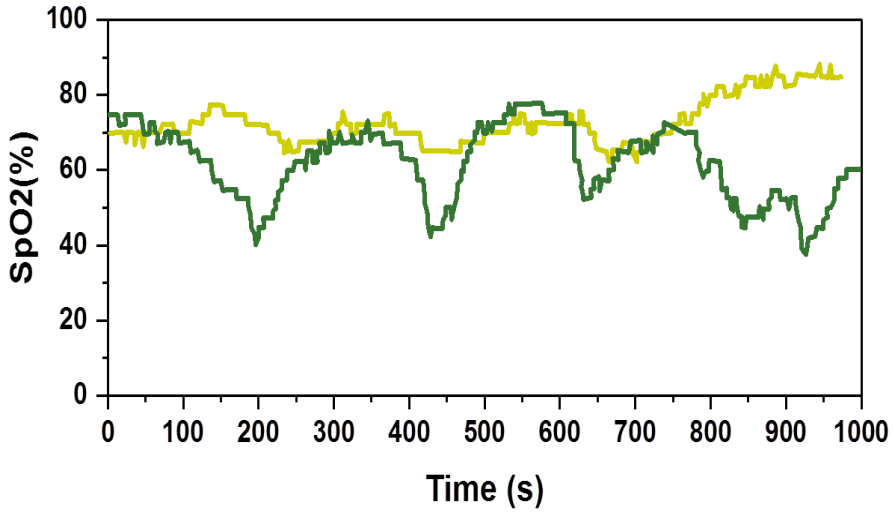

Figure 10. Shows patterns in SpO_2 readings over time.

The area under the curve is called the Area under the Curve (AUC), and it displays the True Positive Rate (Recall) versus the False Positive Rate (1-Specificity) on the Receiver Operating Characteristic (ROC) curve. It shows how well the model can discriminate across classes. A higher AUC indicates improved activity classification accuracy and a decrease in false positives across thresholds. The AUC values of the DGBM model are depicted in **Figure 11**.

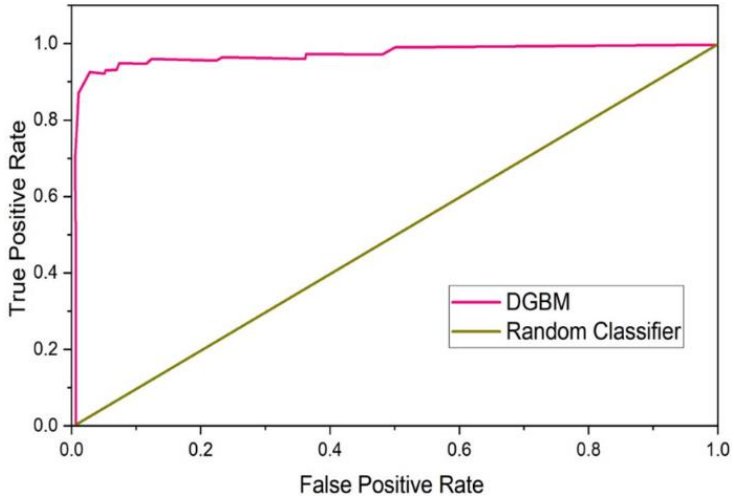

Figure 11. Presents the AUC performance metric of the DGBM model.

Performance analysis with existing methodologies

Accuracy is defined as the relation of appropriately predicted events to all instances. Equation (15) illustrates how well the DGBM model does overall in classifying activities, albeit imbalanced data may make it untrustworthy.

$$Accuracy = \frac{TP + TN}{TP + TN + FP + FN} \times 100 \tag{15}$$

The proposed model is 98.4% higher in accurately detecting the patient's physical activities compared to Random Forest with 1000 trees (RF) [21], Adaboost [21], and gradient boost tree (GBT) [21] are depicted in **Table 4**. The existing RF is 95 % accurately detects patients' activities the adaboost is 94.32% accurately recognizes the patient's physical activities and then the GBT of 95.5 % accurately detects the patient's activities are depicted in **Figure 12a**. **Table 4** compares the performances of four different classification methods in the experiments by taking into account the accuracy, precision, recall, and F1 score. The proposed DGBM method outperformed the rest of the compared methods since it achieved the highest accuracy, precision, recall, and F1 score: 98.4%, 97.9%, 93.1%, and 90.8%, correspondingly.

Table 4. Provides a performance analysis of the system.

Classification methods	Accuracy (%)	Precision (%)	Recall (%)	F1 score (%)
RF	95	94.55	77.45	86.1
Adaboost	94.32	87.72	78.91	83.81
GBT	95.5	94.64	81.87	87.96
DGBM [Proposed]	98.4	97.9	93.1	90.8

The Precision metric quantifies the proportion of correctly anticipated positive cases. It displays the predictive accuracy of the model (e.g., identifying "walking upstairs") when it comes to a particular action or circumstance in Equation (16).

$$Precision = \left(\frac{\mathrm{TP}}{\mathrm{TP} + \mathrm{FP}}\right) \tag{16}$$

The proposed model is 97.9 % positive in predicting the patient's activities compared to the existing RF 94.55% positive predict patients' activities, the AdaBoost is 87.72% positive predict the patient's activities, and the GBT model 94.64 % positive predict the patient's activities in are shown in **Figure 12b**.

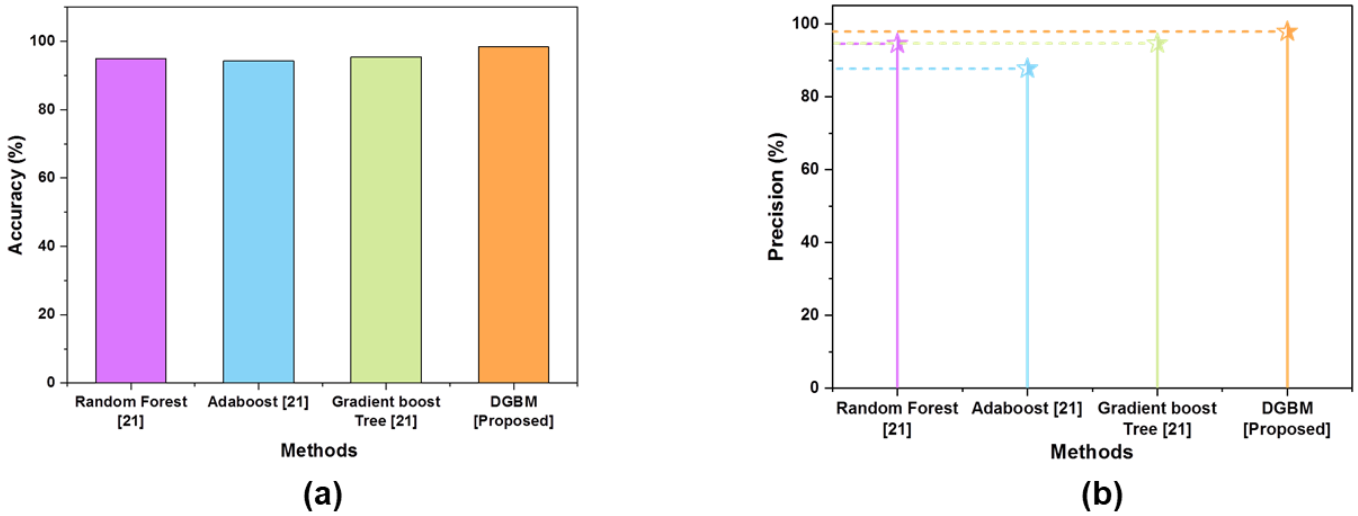

Figure 12. Comparative analysis **(a)** accuracy; **(b)** precision.

The percentage of real positive cases that the model correctly predicted is measured by recall. It shows how well the model can identify all pertinent circumstances or activities (for example, making sure it recognizes the majority of "going downstairs" incidents) depicted in Equation (17).

$$Recall = \left(\frac{\mathrm{TP}}{\mathrm{TP} + \mathrm{FN}}\right) \tag{17}$$

The proposed DGMB model is 93.1% higher in sensitively recognizing the patient's activities compared to the existing RF is 77.45%, the AdaBoost is 78.91% and the GBT model to 81.87% sensitively recognizes the patient's activities are shown in **Figure 13a**.

F1 Score is mainly useful when there is an inequity in classes, is the harmonic mean of Precision and Recall, it guarantees high accuracy as well as a recall for the model, striking a balance between the necessity to locate all pertinent actions and the avoidance of an excessive number of false alarms are illustrated in Equation (18).

$$F1 - Score = 2 \times \left(\frac{\mathrm{Precision} \times \mathrm{Recall}}{\mathrm{Precision} + \mathrm{Recall}}\right) \tag{18}$$

The proposed DGBM model is 90.8% highly optimal balancing the patient's activities compared to the existing RF is 86.1 %, the adaboost is 83.81% and the GBT model to 87.96% optimal balance of the patient activities are shown in **Figure 13b**.

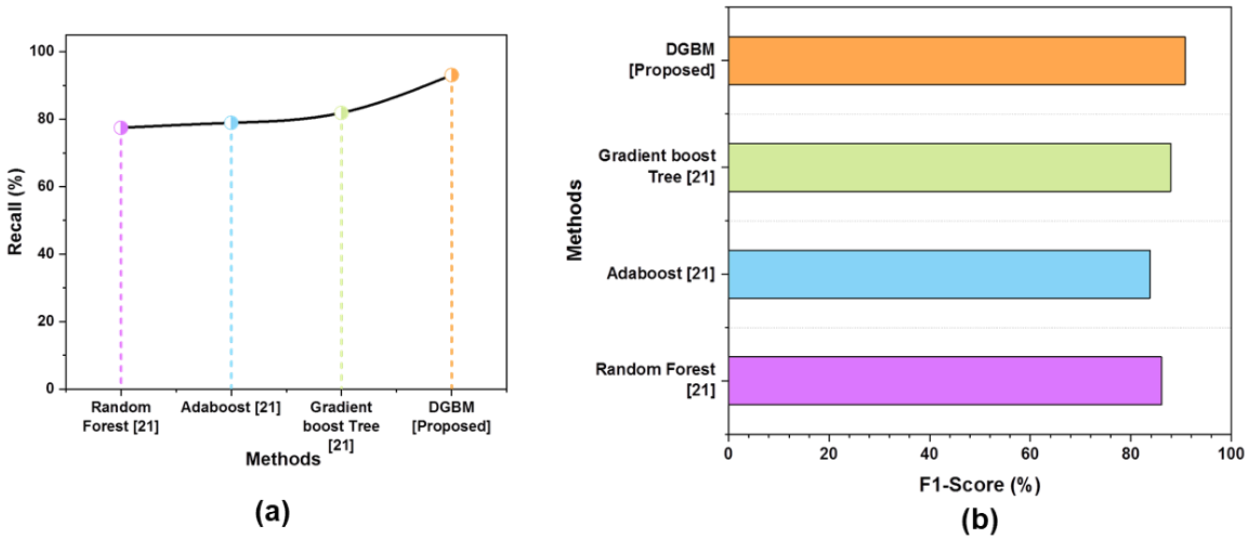

Figure 13. Comparative analysis **(a)** recall; **(b)** f1 score.

5. Discussion

Improving the quality of life of individuals with COPD is one of the best ways to provide them with oxygen as they engage in physical activity. Either Random Forest (RF), Adaboost, or Gradient Boosted Trees (GBT) are the most often used techniques for classifying patient activities and, consequently, regulating oxygen flow. However, there are certain disadvantages to these methods. Adaboost demonstrated somewhat lower accuracy at 94.32% and 87.72%, whereas GBT obtained an accuracy of 95.5% with a precision of 94.64%. The accuracy was 95% with a precision of 94.55%. Notwithstanding the aforementioned impacts of approaches, they seem to fail when it comes to sensitively predicting different ranges of activity levels, adaptability, and particularly when it comes to subtle behaviors like stair climbing. To solve these issues, we suggested incorporating biosensors into the IPOBAB system, which is protected by our Dynamic Gradient Boosted Model (DGBM), which attains a 98.4% classification accuracy and a 97.9% precision. Additionally, DGBM to have superior recall (93.1%) and F1 score (90.8%), whereas other techniques were not consistently reported to be able to detect activity levels and dynamically regulate oxygen flow with respect to needs. By reducing hypoxemia and stabilizing SpO_2 readings, improvements in the DGBM system enable a 40% increase in patient mobility. As the DGBM method's sensitivity and precision rise, it becomes a more practical tool for individualized, real-time oxygen level monitoring.

6. Conclusion

This research introduces an alternate method for creating uninterrupted IPOBAB that without human intervention alters oxygen deliverance in confidence on physical activity level. The device can wirelessly link to the IPOBAB for self-adjustment to a sensor unit that has been formed and weathered to measure the patient's physical activity in real-time. In a methodical experimentation connecting 7 COPD patients, a subjective accuracy of 98.4 %, was reached, patterned blood oxygen saturation readings, and diminishing decompression episodes. Potential

compensation for the not compulsory IPOBAB includes better oxygenation, better patient monitoring, and therapy prescription compliance. Closed-loop oxygen delivery systems can lower healthcare expenses, morbidity and mortality, and medical errors. The median filter reduced noise while maintaining the features of movement. The signal became smoother when the filter eliminated spikes caused by impulse noise. This enhanced patient activity analysis while preserving important data. The improved signal also improved oxygen flow optimization system performance and activity recognition algorithms, leading to more accurate and responsive oxygen therapy based on patient needs as they change in real time. FFT offers advantages such as providing key activity characteristic signals, simplifying physical activity identification, and improving computational efficiency due to its faster computation than traditional methods. The study presents the IPOBAB, which enhances oxygen management during treatment for patients with chronic respiratory illnesses, including COPD, through the use of DGMB algorithms and modern systems for monitoring. To increase the saturation of oxygen and satisfaction with patients, the POBAB employs the DGBM to identify levels of exercise and modify oxygen flow rates depending on real-time SpO_2 values. This is an important achievement in the field of portable oxygen therapy technology. The IPOBAB is a revolutionary system that uses advanced DGBM techniques to monitor and deliver oxygen in real-time. It uses biosensors like SpO_2, pulse rate, and motion sensors to adjust oxygen flow rates based on physical exertion and oxygen saturation levels. The organization optimizes oxygen supply, enhances effectiveness, and improves enduring mobility. It is prepared with medical-grade oxygen concentrators, compressors, and a sophisticated MCU processor. The IPOBAB supports wireless connectivity through BLE and uses MQTT for real-time monitoring and feedback through mobile applications. It can conserve energy while ensuring critical oxygen deliverance during exertion or hypoxemic episodes. Advanced ML methods, such as deep learning (DL) models, could be added to the IPOBAB system to increase the accuracy of its real-time oxygen need forecast. Additionally, it could offer customized patient profiles that could allow tailored treatment. The integration of IoT technologies with the system might enable smooth contact with healthcare providers. Raising the dataset's diversity to encompass more patient demographics might improve the accuracy of the algorithm. Optimizing battery efficiency and downsizing could result in a lighter and more user-friendly system. Clinical trials would offer important insights into the mechanism's long-term safety, effectiveness, and effect on patients' overall QoL.

Ethical approval: Not applicable.

Conflict of interest: The author declares no conflict of interest.

References

1. Sanchez-Morillo, D., Lara-Doña, A., Priego-Torres, B., Morales-Gonzalez, M., Montoro-Ballesteros, F. and Leon-Jimenez, A., 2020. Portable Oxygen Therapy: Is the 6-Minute Walking Test Overestimating the Actual Oxygen Needs? Journal of Clinical Medicine, 9(12), p.4007. DOI: https://doi.org/10.3390/jcm9124007
2. Lellouche, F. and L'Her, E., 2021. Conventional Oxygen Therapy: Technical and Physiological Issues. In High Flow Nasal

Cannula: Physiological Effects and Clinical Applications (pp. 1-36). Cham: Springer International Publishing. https://doi.org/10.1007/978-3-030-42454-1_1

3. Pillai, S., Upadhyay, A., Sayson, D., Nguyen, B.H. and Tran, S.D., 2021. Advances in medical wearable biosensors: Design, fabrication and materials strategies in healthcare monitoring. Molecules, 27(1), p.165. https://doi.org/10.3390/molecules27010165
4. Strapazzon, G., Gatterer, H., Falla, M., Dal Cappello, T., Malacrida, S., Turner, R., Schenk, K., Paal, P., Falk, M., Schweizer, J. and Brugger, H., 2021. Hypoxia and hypercapnia effects on cerebral oxygen saturation in avalanche burial: A pilot human experimental study. Resuscitation, 158, pp.175-182. DOI: https://doi.org/10.1016/j.resuscitation.2020.11.023
5. Verma, D., Singh, K.R., Yadav, A.K., Nayak, V., Singh, J., Solanki, P.R. and Singh, R.P., 2022. Internet of Things (IoT) in nano-integrated wearable biosensor devices for healthcare applications. Biosensors and Bioelectronics: X, 11, p.100153. DOI: https://doi.org/10.1016/j.biosx.2022.100153
6. Wang, L., Lou, Z., Jiang, K. and Shen, G., 2019. Bio‐multifunctional smart wearable sensors for medical devices. Advanced Intelligent Systems, 1(5), p.1900040. DOI: https://doi.org/10.1002/aisy.201900040
7. Swapna, M., Viswanadhula, U.M., Aluvalu, R., Vardharajan, V. and Kotecha, K., 2022. Bio-signals in medical applications and challenges using artificial intelligence. Journal of Sensor and Actuator Networks, 11(1), p.17. DOI: https://doi.org/10.3390/jsan11010017
8. Vakhter, V., Kahraman, B., Bu, G., Foroozan, F. and Guler, U., 2023. A prototype wearable device for noninvasive monitoring of transcutaneous oxygen. IEEE Transactions on Biomedical Circuits and Systems, 17(2), pp.323-335. DOI: https://doi.org/10.1109/TBCAS.2023.3251321
9. Kanna, R.K., Banappagoudar, S.B., Menezes, F.R. and Sona, P.S., 2022, December. Patient Monitoring System for COVID Care Using Biosensor Application. In International Conference on Communication, Networks and Computing (pp. 310-321). Cham: Springer Nature Switzerland. DOI: https://doi.org/10.1007/978-3-031-43140-1_27
10. Kumar, S.A., Gopinath, B., Kavinraj, A. and Sasikala, S., 2021, October. Towards improving patient health monitoring systems using machine learning and the Internet of Things. In 2021 International Conference on Advancements in Electrical, Electronics, Communication, Computing and Automation (ICAECA) (pp. 1-5). IEEE. DOI: https://doi.org/10.1109/ICAECA52838.2021.9675673
11. Mia, M.M.H., Mahfuz, N., Habib, M.R. and Hossain, R., 2021, December. An Internet of Things application on continuous remote patient monitoring and diagnosis. In 2021 4th international conference on bio-engineering for smart technologies (BioSMART) (pp. 1-6). IEEE. DOI: https://doi.org/10.1109/BioSMART54244.2021.9677715
12. Lavric, A., Petrariu, A.I., Mutescu, P.M., Coca, E. and Popa, V., 2022. Internet of Things concept in the context of the COVID-19 pandemic: a multi-sensor application design. Sensors, 22(2), p.503. DOI: https://doi.org/10.3390/s22020503
13. Stella, K., Menaka, M., Jeevitha, R., Jenila, S.J., Devi, A. and Vethapackiam, K., 2023, June. Patient Pulse Rate and Oxygen Level Monitoring System Using IoT. In International Conference on IoT Based Control Networks and Intelligent Systems (pp. 343-355). Singapore: Springer Nature Singapore. DOI: https://doi.org/10.1007/978-981-99-6586-1_23
14. Bhattacharya, S. and Pandey, M., 2022. System for Remote Health Monitoring using Biosensors with IoT Cloud Convergence. NeuroQuantology, 20(16), p.3877. DOI: https://doi.org/10.48047/NQ.2022.20.16.NQ880392
15. Contardi, U.A., Morikawa, M., Brunelli, B. and Thomaz, D.V., 2021. Max30102 photometric biosensor coupled to esp32-webserver capabilities for continuous point-of-care oxygen saturation and heart rate monitoring. Engineering Proceedings, 16(1), p.9. DOI: https://doi.org/10.3390/IECB2022-11114
16. Wong, D.L.T., Yu, J., Li, Y., Deepu, C.J., Ngo, D.H., Zhou, C., Singh, S.R., Koh, A., Hong, R., Veeravalli, B. and Motani, M., 2019. An integrated wearable wireless vital signs biosensor for continuous inpatient monitoring. IEEE Sensors Journal, 20(1), pp.448-462. DOI: https://doi.org/10.1109/JSEN.2019.2942099
17. Jin, X., Liu, C., Xu, T., Su, L., and Zhang, X., 2020. Artificial intelligence biosensors: Challenges and prospects. Biosensors and Bioelectronics, 165, p.112412. DOI: https://doi.org/10.1016/j.bios.2020.112412
18. Nwibor, C., Haxha, S., Ali, M.M., Sakel, M., Haxha, A.R., Saunders, K. and Nabakooza, S., 2023. Remote health monitoring system for the estimation of blood pressure, heart rate, and blood oxygen saturation level. IEEE Sensors Journal, 23(5), pp.5401-5411. DOI: https://doi.org/10.1109/JSEN.2023.3235977
19. Madevska Bogdanova, A., Koteska, B., Vićentić, T., D. Ilić, S., Tomić, M. and Spasenović, M., 2024. Blood Oxygen Saturation Estimation with Laser‐Induced Graphene Respiration Sensor. Journal of Sensors, 2024(1), p.4696031. DOI: https://doi.org/10.1155/2024/4696031

20. Mondal, A., Dutta, D., Chanda, N., Mandal, N. and Mandal, S., 2024. RESPIPulse: Machine learning-assisted sensory device for pulsed mode delivery of oxygen bolus using surface electromyography (sEMG) signals. Sensors and Actuators A: Physical, 369, p.115121. DOI: https://doi.org/10.1016/j.sna.2024.115121
21. Nathan, V., Vatanparvar, K. and Kuang, J., 2020. Assessing Severity of Pulmonary Obstruction from Respiration Phase-Based Wheeze Sensing Using Mobile Sensors. DOI: http://dx.doi.org/10.1145/3313831.3376444